Superficial changes on the Inconel 600 superalloy by picosecond Nd:YAG laser operating at 1064, 532, and 266 nm: Comparative study

J. STAŠIĆ,[1] B. GAKOVIĆ,[1] M. TRTICA,[1] T. DESAI,[2] AND L. VOLPE[3]

[1]VINČA Institute of Nuclear Sciences, University of Belgrade, Belgrade, Serbia
[2]National Research Institute for Applied Mathematics, Jaynagar, Bangalore, India
[3]Universita degli Studi Milano Bicocca, Dipartimento di Fisica "G. Occhialini," Milano, Italy

Abstract

A comparative study of superficial changes on the superalloy Inconel 600, induced by a picosecond Nd:YAG laser operating at 1064, 532, and 266 nm, is presented. All of the laser wavelengths, as well as the used fluences of 2.5 (1064 nm), 4.3 (532 nm), and 0.6 J/cm^2 (266 nm) were found to be adequate for inducing surface variations. Quite different surface features were produced depending on the laser wavelength used. The measured surface damage thresholds were 0.25, 0.13 and 0.10 J/cm^2 for 1064, 532, and 266 nm, respectively. Drastic differences, in function of the wavelength used, were recorded for the crater depths, as well the appearance of hydrodynamic effects and periodic surface structures. Differences in crater depths were explained via an easier propagation of the first harmonic laser radiation (1064 nm) through the ejected material and plasma compared to a radiation at 532 and 266 nm. Finally, changes in the surface oxygen content caused by ultrashort laser pulses were considered.

Keywords: Laser ablation; Periodic surface structures; superalloy Inconel; Surface morphology

1. INTRODUCTION

Nickel-based superalloy are in a class of special alloys characterized by extraordinary properties. These alloys possess high temperature and mechanical strength, great corrosion resistance, especially at elevated temperatures, outstanding resistance to pitting, good heat conductivity, resistance to aggressive atmosphere (e.g., acids). Due to these excellent features, the alloys are attractive for numerous applications in electrical, chemical and food industry, aero and space engineering, etc. Moreover, superalloy can be used in the nuclear complex, in the technology of fission as well as fusion reactors (In *et al.*, 1995; Busharov *et al.*, 1977). Thus, the quality of fusion plasma in a thermonuclear device depends not only on the reactor design, but also on the proper selection of reactor vessel wall material, especially plasma facing materials (Sannazzaro *et al.*, 1991). Nickel-based superalloy Inconel 600, high quality steels, etc., can be used as plasma facing materials. These materials are, among other, exposed to fluxes of electromagnetic radiation in the reactor so their behavior can be simulated in the laboratory using high intensity laser radiation. Inconel superalloy was recently successfully applied in medicine as an implant for cardiovascular usage (Grifka *et al.*, 2008). It is well known that the implant surface, as well as its state, influences the level of biocompatibility with human body. One of the promising treatments of implants, including Inconel 600, is laser treatment. Finally, specific applications, e.g., aerospace engineering, require perforation of small apertures which, apart from conventional techniques, can be achieved by lasers (Chen & Liu, 1999).

Generally, surface modifications of different nickel-based superalloys using laser systems are of great fundamental and practical interest. Studies on the interaction of laser beam with these alloys were intensified in the last decade. Various laser systems, such as pulsed Nd:YAG (Chen *et al.*, 1996; Bugayev *et al.*, 2006), excimer (Pantelis & Psyllaki, 1996), pulsed and continues wave CO_2 (Zysk, 1990; Hong *et al.*, 2008) and Ti:sapphire lasers have been used for these purposes (Feng *et al.*, 2005; Semaltianos *et al.*, 2009).

Investigations of the interaction of pulsed picosecond laser beam with nickel-based superalloys particularly Inconel 600, which is just the focus of this research, are scarce in literature.

Address correspondence and reprint requests to: Jelena Stašić, VINČA Institute of Nuclear Sciences, P.O. BOX 522, 11001 Belgrade, Serbia. E-mail: jelsta@vinca.rs

Superalloy Inconel 600 surface changes induced by pulsed picosecond Nd:YAG laser emitting in the near-infrared (1064 nm), visible (532 nm), and ultraviolet spectral domain (266 nm) were the main goal of this study. The accent in this work is on the studies of morphological features of the target. This research is essentially fundamental, but can be of a great use since the laser enables quick heating and cooling cycles, which can cause interesting transformations, e.g., rapid phase transitions. One of the potential applications is a very precise aperture creation, which is necessary in a large number of applications.

2. EXPERIMENTAL

The Inconel 600 samples used in these investigations were of rectangular shape with dimensions 15 mm × 25 mm × 2 mm (width × length × thickness). Surface of the samples was prepared before irradiation by a standard metallographic procedure. The samples were mechanically polished (first by using SiC grinding paper (360–1200 grit) and finally by using diamond paste (1–0.25 μm)), ultrasonically cleaned and dried in hot air. Prior to laser irradiation they were cleaned in ethanol. Typical initial surface roughness was around 100 nm. The experimental setup used in this work is described in Gakovic et al. (2007), but for the sake of completeness some details will be given. The laser utilized for irradiation was a picosecond Nd:YAG laser system, model SYL P2, produced by QuantaSystem Srl.-Solbiate. This laser is an active-passive mode-locked Nd:YAG system. It includes a laser oscillator, an amplifier, and a nonlinear crystal (KD*P). Pulse duration of about 40 picoseconds is obtained by using a saturable absorber dye and an acousto-optic standing wave modulator. Further, it possessed possibility to emit radiation at first, second, or fourth harmonic. Typical laser output parameters during the experiments are given in Table 1.

Samples were irradiated by focusing the laser beam using a quartz lens of 12 cm focal length. During the irradiation process, the laser was operated in the near single frequency mode. The angle of incidence of the laser beam with respect to the surface was about 90°. Irradiation was carried out in air, at a pressure of 1013 mbar and standard relative humidity.

Table 1. *Typical parameters of the picosecond Nd:YAG laser used during irradiation of Inconel 600 target*

Laser wavelength, λ	1064 nm	532 nm	266 nm
Pulse duration, τ	40 ps		
Pulse energy, E_p	≤8.3 mJ	≤30 mJ	≤5 mJ
Laser fluence, Φ	≤2.5 J/cm^2	≤4.3 J/cm^2	≤0.6 J/cm^2
Laser intensity, I	≤10^{12} W/cm^2		
Pulse repetition rate, f	2 Hz		
Polarization	Linear, p polarization		
Mode structure	Near TEM$_{00}$		

Laser energy was attenuated with the combination of neutral density (ND) filters keeping the input energy constant.

Various analytical techniques were used for characterization of the Inconel 600 prior to and after picosecond laser irradiation. Surface morphology was monitored by optical and scanning electron microscopy (SEM). SEM was coupled to an energy-dispersive analyzer (EDX) for determining the sample surface composition. A profilometer (Taylor-Hobson Talysurf 2) was used for specifying the geometry of the damaged/ablated area.

3. RESULTS AND DISCUSSION

Surface of the Inconel 600 had a typical silver-gray metallic color before irradiation. EDX elemental analysis of the sample surface before irradiation showed the following content: nickel (~57.2 wt.%), balanced to a 100% by C (5.0 wt.%), O (~3.1 wt.%), Al (~0.7 wt.%), Si (~0.7 wt.%), Cr (~10.4 wt.%), Fe (~10.4 wt.%) and, Mo (~12.4 wt.%). Complete elemental analysis was normalized.

Investigations of the morphological changes induced by picosecond laser on the Inconel 600 target have shown their dependence on the laser beam characteristics, primarily on the laser fluence, peak power density, wavelength and number of accumulated pulses.

Topographical features of the Inconel 600 surface were primarily observed in function of the laser wavelength used, i.e. at three wavelength operational laser regimes: first (1064 nm), second (532 nm), and fourth (266 nm) harmonic regime. All three wavelengths induced surface changes of the Inconel 600. The results of the induced surface modification are presented in the following text.

3.1. Regime of a Laser Emission at 1064 nm

Pulse energy of a picosecond Nd:YAG laser used in this wavelength regime was 8.3 mJ. Thus, the laser energy density (fluence), based on the calculation using $1/e^2$ diameter of a Gaussian beam (~600 μm), was 2.5 J/cm^2. Corresponding intensity of the laser radiation was $0.6 \cdot 10^{11}$ W/cm^2. Morphological changes on the target surface caused by the action of 1, 5 and 50 pulses are shown in Figures 1 and 2. Modifications of the Inconel 600 surface, induced by picosecond laser operating at 1064 nm, can be summarized as follows: (1) appearance of the craters, Figures 1A1, 1A2, 1A3, (2) appearance of the hydrodynamic effects particularly prominent after irradiation with 5 and 50 laser pulses, Figures 1A2, 1A3, 1C2, 1C3, 1D3, and (3) appearance of the specific self-organized structures at submicron dimensions, Figure 1D1, as well as characteristic holes at the periphery (Fig. 1D2).

Damage threshold, defined as a minimum laser radiation density necessary for the creation of a detectable damage on the material, was determined. Keeping the number of laser pulses constant at four and slowly lowering the laser energy it was observed that the last visible damage
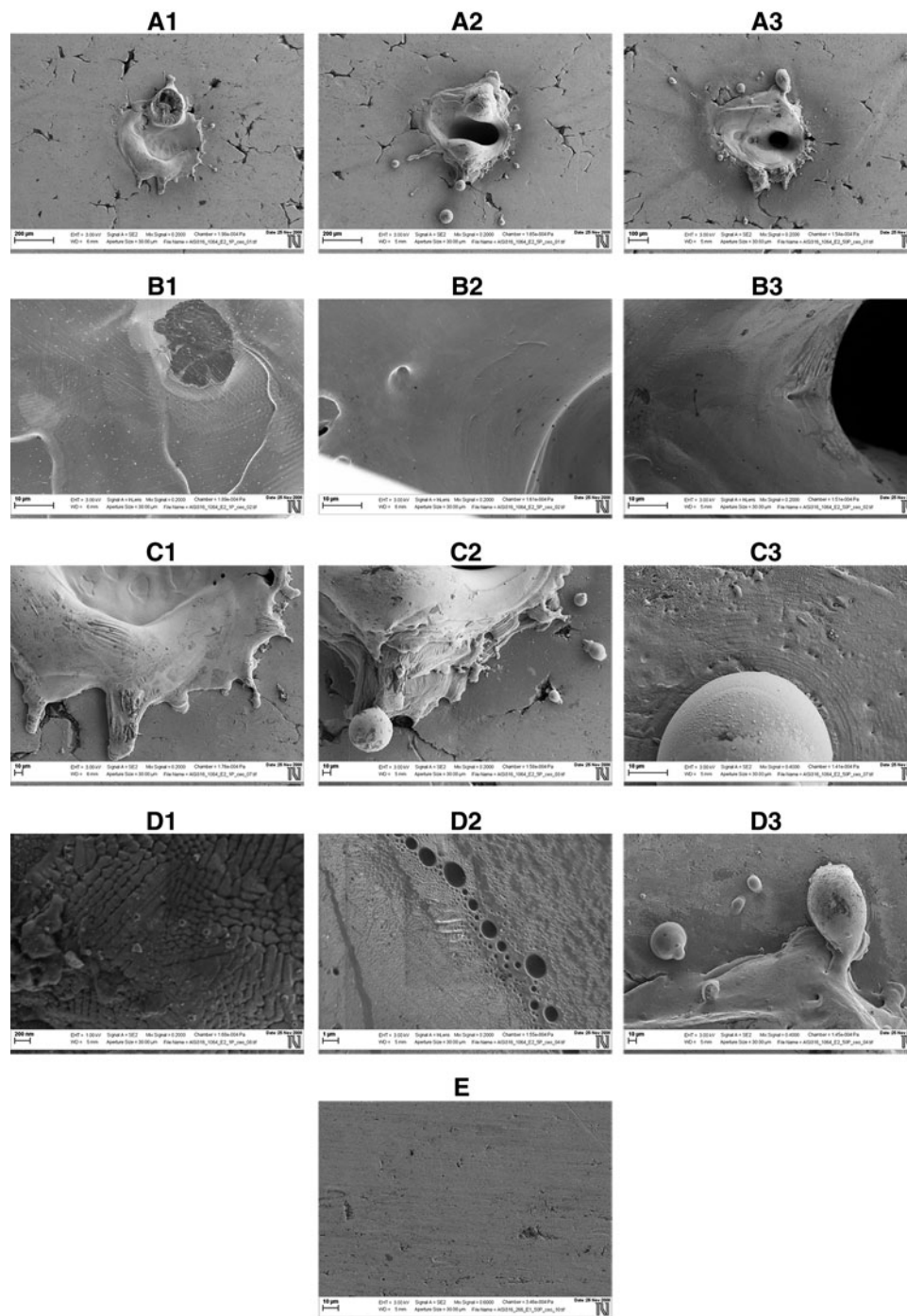
Fig. 1. SEM analysis of the Inconel 600 surface after irradiation by picosecond Nd:YAG laser at $\lambda = 1064$ nm, fluence 2.5 J/cm^2. (A1–D1): after 1 pulse, (A2–D2): after 5 pulses, (A3–D3): after 50 pulses, E = view of the target prior to irradiation (B = center, C and D = periphery of the irradiated area).

occurs at the total delivered energy of 0.037 mJ, so the damage threshold was evaluated to be around 0.25 J/cm^2 using the spot diameter of about 140 µm obtained from optical micrographs. There is no data available in the literature on the damage threshold of the Inconel 600 affected by picosecond laser; however our results are in a good accordance with the results for other types of nickel-based

superalloys. For instance, single pulse damage threshold in case of the picosecond laser at 1064 nm acting on the superalloy C263, is equal to 0.68 ± 0.02 J/cm^2 (Semaltianos *et al.*, 2010). This is in a good accordance with our result, since it has been established that the damage threshold decreases in case of multiple pulse accumulation (Semaltianos *et al.*, 2009). Damage threshold obtained in our work approximates
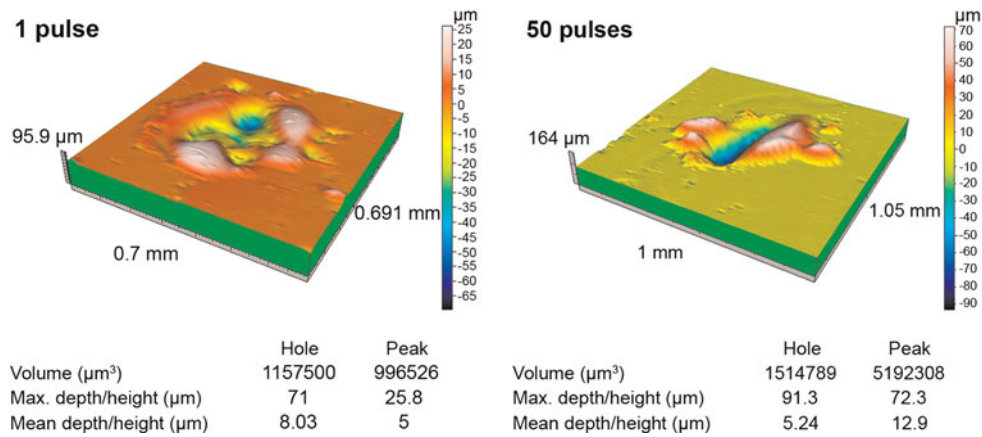
Fig. 2. (Color online) The view of the Inconel 600 surface after irradiation with 1 and 50 pulses of picosecond Nd:YAG laser at $\lambda = 1064$ nm. Profilometric analysis; fluence, 2.5 J/cm^2.

to the single pulse damage thresholds of about 0.3 J/cm^2 for nickel-based superalloys irradiated with femtosecond laser pulses (Feng *et al.*, 2005; Semaltianos *et al.*, 2009).

During laser interaction with metals, including Inconel 600, the laser energy is absorbed primarily by free electrons (Bauerle, 2003; Chichkov *et al.*, 1996). The absorbed radiation energy in the skin layer involves thermalization of electrons. Part of the electron energy is transferred into the bulk in the form of heat, while the later part is transferred to the lattice subsystem. In the first case, the electron diffusion process is essential. Finally, if the initial laser fluence is sufficient, surface damaging/ablation can take place. For laser pulses with fluences higher than the damage threshold, thermal diffusivity cannot be neglected. Depending on the fluence, a series of effects such as melting, vaporization of the molten material, dissociation, and ionization of the vaporized material, etc., can be generated on the target. In our experiments, Inconel 600 was irradiated with lower fluence, 2.5 J/cm^2, which resulted in lower damage/ablation rate. Morphological changes, such as micro-droplets and micro-cracking, were mainly a consequence of a rapid heating and cooling of the target surface layer (Figs. 1C1–1C3, 1D3). Probably one transition phase — liquid phase, is present here. The process of Nd:YAG laser interaction with Inconel 600 during the first and subsequent pulses was accompanied by the appearance of plasma in front of the sample. Shape of the plasma was somewhere in between the so-called "torch" and the "spark" form. Generally, the

role of the plasma for pulses in pico- and nanosecond time domain, contrary to the femtosecond time domain, is of high importance. Recent investigations showed that the first stage of plasma in front of the target was obtained after about 20 ps (Mao *et al.*, 2000) whereas its full development occurs after several hundreds of picoseconds to several nanoseconds. In this case, the influence of the plasma on laser radiation propagation must be taken into account. For femtosecond pulses, the situation is better because the laser pulse is terminated before the plasma development in front of the target.

The three-dimensional view of the Inconel 600 surface after-irradiation with 1 and 50 pulses of the fluence 2.5 J/cm^2 is given in Figure 2. For this characterization, the profilometer was used. Numerical data concerning craters shown in Figure 2 — crater volume, volume of the surrounding ejected material, and maximum crater depths, are given in Table 2. Generally, for 1 and 50 applied laser pulses, the difference in crater parameters, Table 2, is evident. Crater volume and its maximum depth, as well as the volume of the ejected material, are higher in case of 50 accumulated pulses.

Table 2. *Crater parameters obtained by profilometric analysis of the Inconel 600 target surface at $\lambda = 1064$ nm, fluence 2.5 J/cm^2*

Crater parameters	1 pulse	50 pulses
V_{crater} [μm^3]	1157500	1514789
$V_{ejected}$ [μm^3]	996526	5192308
Max. depth [μm]	71	91.3

Table 3. *EDX analysis of the spot irradiated with 1 pulse of picosecond Nd:YAG laser at $\lambda = 1064$ nm and fluence $\Phi = 2.5$ J/cm^2; spectrum 1 = center of the irradiated area, spectrum 2 = periphery of the irradiated area, spectrum 3 = non-irradiated zone*

Element	Spectrum 1 [wt%] (center)	Spectrum 2 [wt%] (periphery)	Spectrum 3 [wt%] (before irradiation)
C	18.47	16.33	5.01
O	0.81	2.19	3.10
Al	0.54	0.62	0.67
Si	0.24	0.27	0.76
Cr	9.27	9.47	10.40
Fe	8.83	8.70	10.43
Ni	53.36	52.34	57.21
Mo	8.48	10.09	12.42
Total	~100		

Irradiation of the Inconel 600 target was performed in the air atmosphere; therefore variations in the oxygen content on the surface are quite possible. Monitoring of the target constituents, especially oxygen, before and after the action of 1 pulse at the laser fluence $\Phi = 2.5$ J/cm^2, is shown in Table 3. EDX method was used for this purpose and the analysis was carried out at three locations — periphery, central damage zone, as well as the non-irradiated region. Generally, irradiation of the sample with picosecond laser, at the fluence of 2.5 J/cm^2, resulted in the changes of oxygen concentration. Its concentration decays from the damage periphery towards the centre compared to a non-irradiated area, which implies the removal of oxides from the target surface. Also, content of the nickel is decreased while the carbon concentration is higher, which could be interpreted as a formation of nickel carbide on the irradiated surface.

3.2. Regime of a Laser Emission at 532 nm

During irradiation of the Inconel 600 target with the laser wavelength of 532 nm, pulse energy was 29.7 mJ, energy density (fluence) 4.3 J/cm^2 (spot diameter $\sim$900 μm), and the radiation intensity about 10^{11} W/cm^2.

Morphological changes on the target after laser irradiation are shown in Figures 3 and 4 and they can be summarized as follows: (1) appearance of the superficial damage with the presence of surrounding aureola, (2) appearance of grainy structure (Fig. 3B3), as well as accumulation of the ablated material in nano-grain forms (central zone), Figures 3C1, 3C2; (3) development of periodic surface structures (PSS) in micro- and nano-domain. These structures are present at near and further periphery. Irradiations of the target with this fluence were also accompanied by the occurrence of plasma in front of the target.
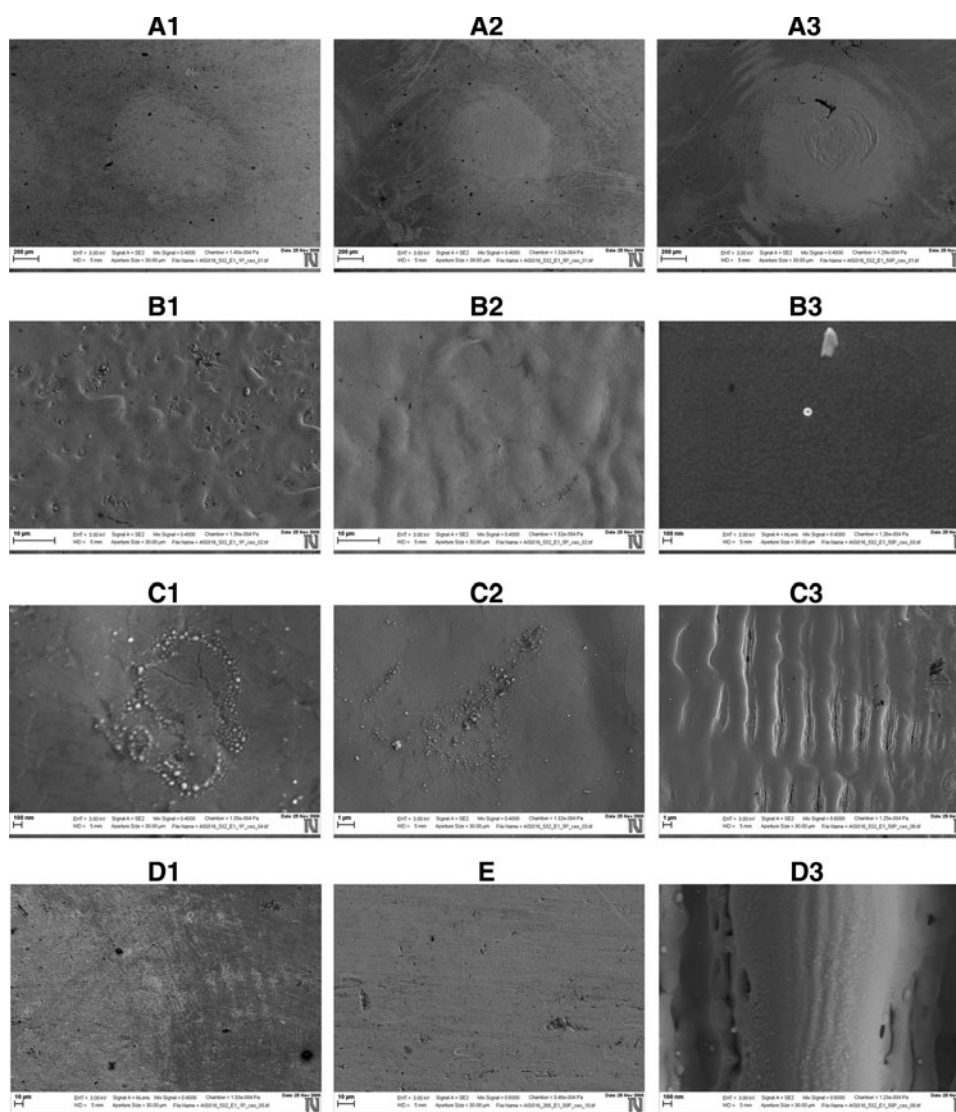

Fig. 3. SEM images of the Inconel 600 after irradiation with picosecond Nd:YAG laser at λ = 532 nm, fluence, 4.3 J/cm^2. (A1–D1): after 1 pulse, (A2–C2): after 5 pulses, (A3–D3): after 50 pulses, E = non-irradiated area. B, C1, C2 = center; C3, D1, D3 = periphery of the irradiated spot. (C3, D3 = periodic surface structures).
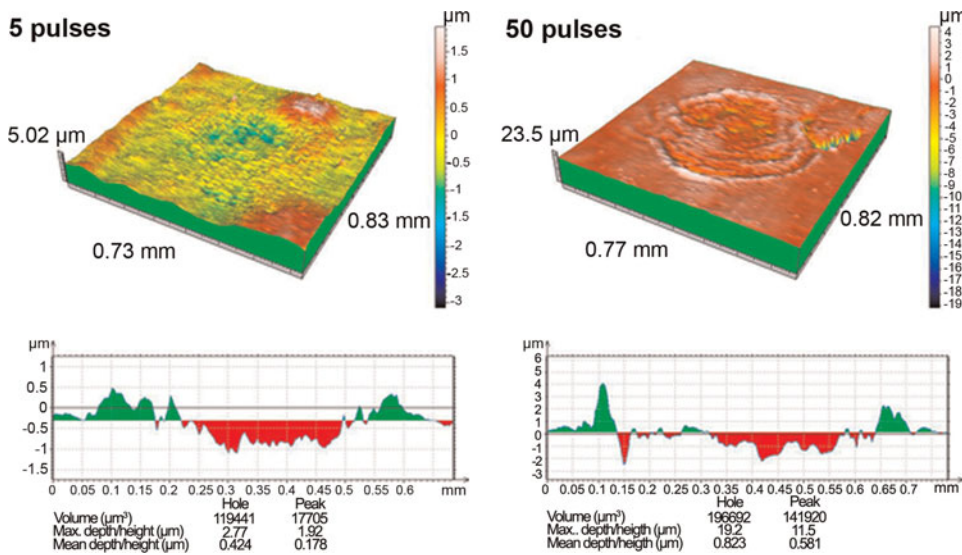
Fig. 4. (Color online) Profilometric analysis of the Inconel 600 superalloy after irradiation with 5 and 50 pulses of picosecond Nd:YAG laser at $\lambda = 532$ nm fluence, 4.3 J/cm^2.

From the analysis of the periodic surface structures, it can be concluded that they were typically formed after 50 laser pulses (Fig. 3). Periodicity of the micro-domain structures was about 3–4 μm (Fig. 3C3). These ripples are present over the entire area of nano-domain structures with the periodicity around 200 nm. It can be assumed that the micro-domain structures are a result of thermal wrinkling, while nano-domain ripples occur due to the interference of the incoming laser beam with the so called surface waves (Tan & Venkatakrishnan, 2006).

Surface damage threshold was also evaluated using the same experimental procedure as described for 1064 nm wavelength. Minimum laser energy that induced damage was 0.044 mJ, number of pulses $N = 1$. Using damage diameter of about185 μm, estimated from the optical microscope images, the calculated damage threshold is about 0.16 J/cm^2. This is lower than the value obtained at 1064 nm, which is probably a consequence of higher absorption of the target at 532 nm.

The three-dimensional view of the Inconel 600 surface after irradiation with 5 and 50 pulses at the fluence of 4.3 J/cm^2 is shown in Figure 4. The damages are superficial and the depth of the irradiated parts was approximately 1 and 2 μm.

EDX analysis of the elements on the surface after irradiation with one pulse at $\lambda = 532$ nm showed that the entire irradiated area has somewhat lower oxygen concentration, decaying from the periphery towards the center, compared to a non-irradiated material. Decrease of the oxygen concentration is higher compared to the laser wavelength of 1064 nm.

3.3. Regime of a Laser Emission at 266 nm

During irradiation of the Inconel 600 target with the laser wavelength of 266 nm and pulse energy of 4.65 mJ, the fluence and radiation intensity were 0.6 J/cm^2 (spot diameter ~ 1000 μm) and 0.2×10^{11} W/cm^2, respectively. Morphological changes induced after 1, 5 and 50 pulses at 266 nm are presented in Figures 5 and 6. Energy density of 0.6 J/cm^2 caused surface modifications on the superalloy target. Generally, surface phenomena during laser action at 266 nm are the following: (1) surface ablation of the material with three distinct zones — center, near and further periphery (aureola); (2) appearance of "holes," i.e., local boiling centers and, locally, redeposited nano-spheres in the central area (Fig. 5B,C); (3) presence of the periodic surface structures on the periphery, and (4) formation of spark plasma in front of the target after first few pulses due to high intensity radiation.

Periodic surface structures occurred already after one as well as after 5 and 50 pulses (Fig. 5E). Generally, they become more prominent with accumulation of laser pulses. Dimensions of the obtained PSS are on the nanometer scale, and their periodicity is approximately 250–300 nm after 50 pulses, which is approximately in accordance with the laser wavelength. Dependence of the periodicity of such structures (Λ) on the laser wavelength is given with:

$$\Lambda \approx \frac{\lambda_{\text{laser}}}{\cos \theta_i} \quad p\text{-polarization,}$$
$$\Lambda \approx \frac{\lambda_{\text{laser}}}{1 \pm \sin \theta_i} \quad s\text{-polarization,}$$

(1)

where θ_i denotes the incident angle of the beam (Tan & Venkatakrishnan, 2006; Trtica *et al.*, 2009). In this case, the beam had a linear horizontal polarization, and the angle of incidence with respect to the sample surface was near normal, $\Delta\theta \sim \pm 3°$. The measured values for the periodicity in this work agree with the predictions of Eq. (1) in case of *p*-polarized beam.

Approximate damage threshold for picosecond Nd:YAG laser-superalloy Inconel 600 interaction was determined after the accumulation of eight pulses with total energy 0.129 mJ, and is equal to 0.10 J/cm^2 (damage diameter ~
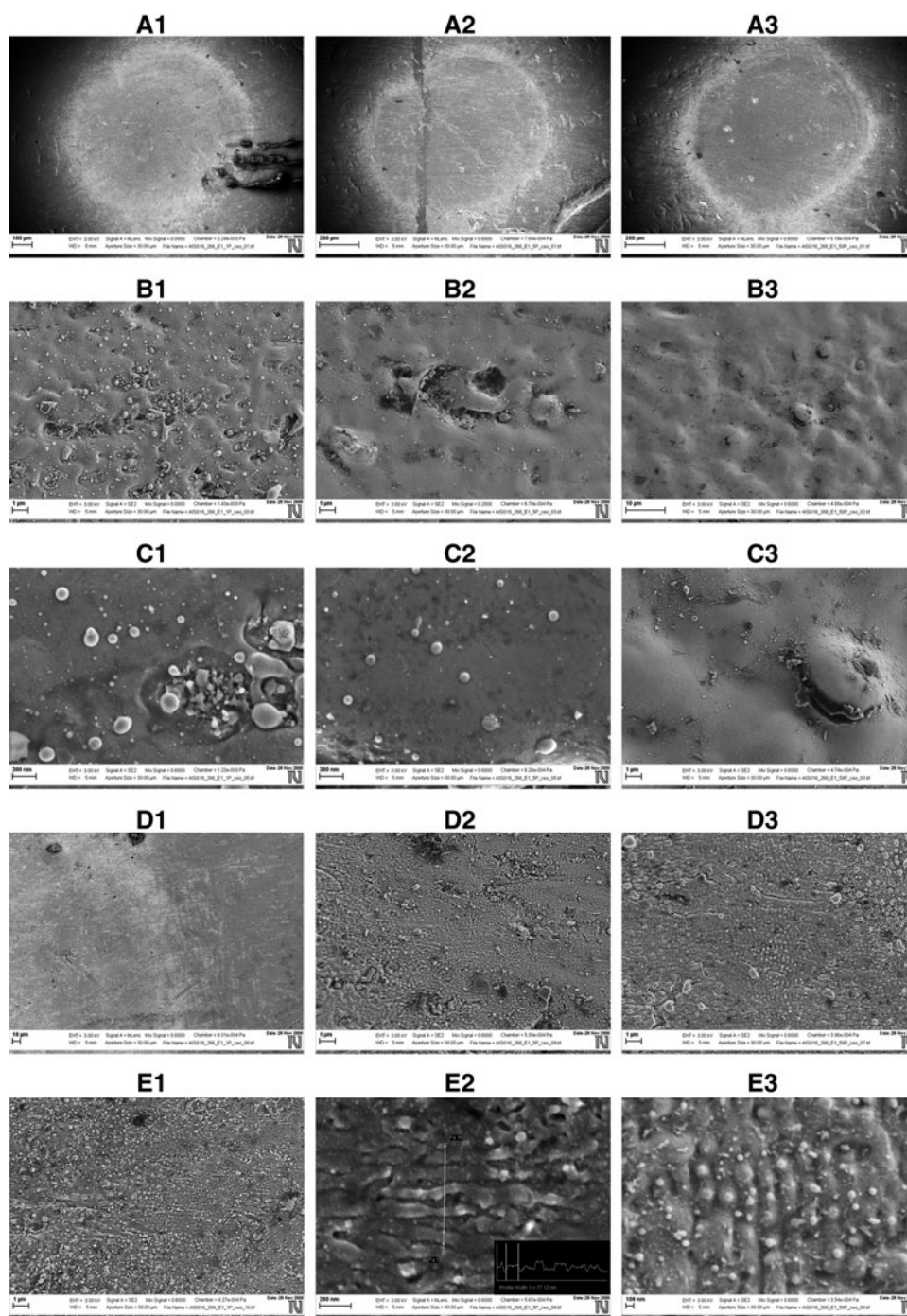
Fig. 5. SEM micrographs of the Inconel 600 target after irradiation with picosecond Nd:YAG laser at $\lambda = 266$ nm, fluence, 0.6 J/cm^2. (A1–E1): after 1 pulse, (A2–E2): after 5 pulses, (A3–E3): after 50 pulses. B, C = center; D, E = periphery of the irradiated area (E2, E3 = periodic surface structures).

400 μm). Damage threshold data in case of laser working at 266 nm with pulses in picosecond time domain are scarce in literature.

Profilometric analysis of the superalloy Inconel 600 after irradiation with 1 and 50 laser pulses with the fluence 0.6 J/cm^2 is given in Figure 6. Damage depth was of the order of microne. Unlike the formation of craters after the action

of first laser harmonic damages are, similar to irradiation at the laser wavelength of 532 nm, superficial. It can be assumed, based on the data for neat nickel (Cabalin & Laserna, 1998), that the absorption of laser radiation at 266 nm and 532 nm by the target surface is higher compared to the first harmonic; therefore deeper damages on these wavelengths would be expected. A possible explanation for this
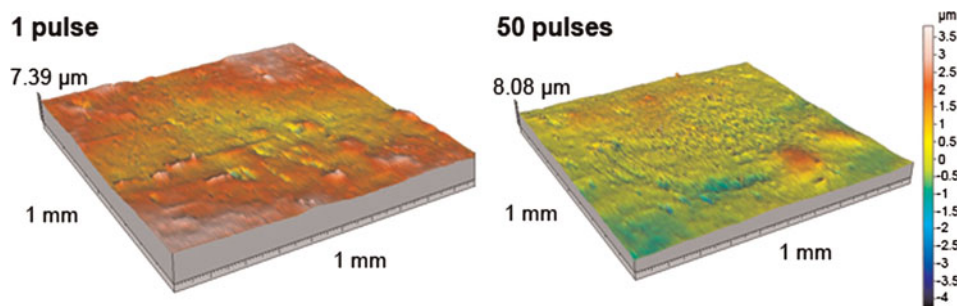
Fig. 6. (Color online) Profilometer analysis of the superalloy Inconel 600 target after irradiation with 1 and 50 pulses of picosecond Nd:YAG laser at $\lambda = 266$ nm and fluence $\Phi = 0.6$ J/cm^2.

phenomenon is an easier propagation of the beam at 1064 nm through the ejected material and plasma formed in front of the sample. Namely, it was shown that the absorption of laser radiation by plasma strongly depends on the laser wavelength and is much higher, for example, in the visible than in the infrared spectral area (Abdellatif & Imam, 2002). Due to this, coupling of the laser energy at the second and fourth harmonic with the material is weakened and the effect is known as the "plasma shielding" (Mao *et al.*, 1993).

EDX chemical analysis of the Inconel 600 surface after irradiation with one pulse was also conducted. Three locations at the surface were analyzed — center, periphery, and non-irradiated area. Decrease of the oxygen concentration from the non-irradiated area via periphery to the central zone was registered. Generally, lower level of the oxygen content in the periphery as well as the central irradiated zone compared to the wavelength of 1064 nm was recorded.

4. CONCLUSION

A comparative study of the superficial changes on the superalloy Inconel 600, induced by a picosecond Nd:YAG laser operating at 1064, 532, and 266 nm, is presented. It was shown that all laser wavelengths, as well as the used fluences of 2.5 (1064 nm), 4.3 (532 nm), and 0.6 J/cm^2 (266 nm) were sufficient for inducing surface modifications. Comparative results obtained by three wavelengths in ultrashort time domain are given in Table 4. It

can be clearly seen from this table that the picosecond laser produces different surface features in these three regimes. Thus, among other, a drastic difference between the damage depths at all three wavelengths used is recorded. The crater depth for 1064 nm is about two orders higher with respect to the depths obtained at 532 or 266 nm. Also, the difference in the damage threshold is evident. Formation of the craters approximately one hundred times deeper at 1064 nm is explained via easier propagation of the first harmonic radiation through the ejected material and plasma compared to radiation at 532 and 266 nm. In case of second and fourth harmonic action on the target, accumulation of nano-spheres in the damage centre occurs. Appearance of the hydrodynamic effects was recorded only for the wavelength of 1064 nm, while the periodic surface structures were registered only at 532 and 266 nm. In case of 532 nm, PSS are on micrometer as well as nanometer scale, while at 266 nm only nm-PSS were present. Chemical analysis showed that all three wavelengths efficiently clean oxides from the surface.

Comparing the results obtained in this work with our previous paper on femtosecond laser modification of Inconel, it can be concluded that high repetition fs pulses give smaller damage diameters and the ablation is cleaner. However, contrary to ps laser, the effect of periodic surface structures was not observed. Also, the picosecond laser system is desirable from the economic point of view, and provides aperture diameters small enough for many applications.

Table 4. *Comparative summary effects induced on the Inconel 600 target by picosecond Nd:YAG laser at λ = 1064, 532 and 266 nm*

1064 nm	532 nm	266 nm
Formation of craters, 2.5 J/cm^2 depth ∼90 μm (1 pulse)	Surface damages, 4.3 J/cm^2 depth ≤1.0 μm (5 pulses) depth ≤2.0 μm (50 pulses)	Surface damages, 0.6 J/cm^2 depth ∼1.0 μm (for both 20 and 50 pulses)
Damage threshold 0.25 J/cm^2	Damage threshold 0.13 J/cm^2	Damage threshold 0.10 J/cm^2
"Holes" (local boiling centers) in the central zone; grainy structure at the periphery.	(i) Large melted areas; (ii) grainy structure after 50 pulses; (iii) accumulated nano-spheres in the central zone.	(i) Large melted areas; (ii) "holes" (local boiling centers); (iii) accumulated nano-spheres in the central zone.
Hydrodynamic features	Rare hydrodynamic features	Rare hydrodynamic features
Decrease of the oxides in center and periphery	Decrease of the oxides from the periphery towards center	Decrease of the oxides from the periphery towards center
No PSS	PSS after 50 pulses with the periodicity: (i) ∼3–4 μm on μm-scale; (ii) ∼200 nm on nm-scale	PSS on nm-scale after 1, 5 and 50 pulses, with the periodicity ∼150 nm (5 pulses) and 200–250 nm (50 pulses)

As can be seen from our experiments wavelength of 1064 nm is favourable for processing applications, such as drilling and cutting. On the other hand, 532 nm and 266 nm are more suitable for finer surface modifications, e.g. formation of periodic surface structures. These structures can be applied in medicine (increasing the implant roughness), optics (dispersive elements), etc.

ACKNOWLEDGMENTS

REFERENCES

ABDELLATIF, G. & IMAM, H. (2002). A study of the laser plasma parameters at different laser wavelengths. *Spectrochim. Acta Part B* **57**, 1155–1165.

BÄUERLE, D. (2003). Thermal, photophysical, and photo chemical processes. In *Laser Processing and Chemistry*. Berlin: Springer Verlag.

BUGAYEV, A.A., GUPTA, M.C. & PAYNE, R. (2006). Laser processing of Inconel 600 and surface structure. *Opt. Lasers Engin.* **44**, 102–111.

BUSHAROV, N.P., GUSEV, V.M., GUSEVA, M.I., KRASULIN, YU.L., MARTYNENKO, YU.V., MIRNOV, S.V. & ROZINA, I.A. (1977). Sputtering and blistering in the bombardment of inconel, Sic + C alloy, and carbon-pyroceramic by H^+ and He^+ ions. *At. Energy* **42**, 554–559.

CABALIN, L.M. & LASERNA, J.J. (1998). Experimental determination of laser induced breakdown thresholds of metals under nanosecond Q-switched laser operation. *Spectrochim. Acta Part B* **53**, 723–730.

CHEN, X. & LIU, X. (1999). Short pulsed laser machining: how short is short enough. *J. Laser Appl.* **11**, 268–272.

CHEN, X., LOTSHAW, W., ORTIZ, A.L., STAVER, P.R., ERIKSON, C.E., MCLAUGHLIN, M.H. & ROCKSTROH, T.J. (1996). Laser drilling of advanced materials: effects of peak power, pulse format, and wavelength. *J. Laser Appl.* **8**, 233–239.

CHICHKOV, B.N., MOMMA, C., NOLTE, S., VON ALVENSLEBEN, F. & TÜNNERMANN, A. (1996). Femtosecond, picosecond and nanosecond laser ablation of solids. *Appl. Phys. A* **63**, 109–115.

FENG, Q., PICARD, Y.N., LIU, H., YALISOVE, S.M., MOUROU, G. & POLLOCK, T.M. (2005). Femtosecond laser micromachining of a single-crystal superalloy. *Scripta Mater.* **53**, 511–516.

GAKOVIC, B., TRTICA, M., BATANI, D., DESAI, T., PANJAN, P. & VASILJEVIC-RADOVIC, D. (2007). Surface modification of titanium nitride film by a picosecond Nd:YAG laser. *J. Opt. A* **9**, 76–80.

GRIFKA, R.G., FENRICH, A.L. & TAPIO, J.B. (2008). Transcatheter closure of patent ductus arteriosus and aorto-pulmonary vessels using non-ferromagnetic Inconel MReye embolization coils. *Cathet.Cardiovasc. Interventions* **72**, 691–695.

HONG, J.K., PARK, J.H., PARK, N.K., EOM, I.S., KIM, M.B. & KANG, C.Y. (2008). Microstructures and mechanical properties of Inconel 718 welds by CO_2 laser welding. *J. Mater. Proc. Techn.* **201**, 515–520.

IN, C.B., KIM, Y.I., KIM, W.W., KIM, J.S., CHUN, S.S. & LEE, W.J. (1995). Pitting resistance and mechanism of TiN-coated Inconel 600 in 100°C NaCl solution. *J. Nucl. Mater.* **224**, 71–78.

MAO, S.S., MAO, X.L., GREIF, R. & RUSSO, R.E. (2000). Simulation of a picosecond laser ablation plasma. *Appl. Phys. Lett.* **76**, 3370–3372.

MAO, X.L., CHAN, W.T., SHANNON, M.A. & RUSSO, R.E. (1993). Plasma shielding during picosecond laser sampling of solid materials by ablation in He versus Ar atmosphere. *J. Appl. Phys.* **74**, 4915–4922.

PANTELIS, D. & PSYLLAKI, P. (1996). Excimer laser micromachining of CMSX2 and TA6V alloys. *Mater. Manuf. Proc.* **11**, 271–282.

SANNAZZARO, G., SBORCHIA, C., SONNERUP, L. & HUGUET, M. (1991). Low cycle fatigue testing of Inconel 600 and life assessment of JET vacuum vessel. *Proceedings of 14th IEEE/NPSS Symposium on Fusion Engineering*. San Diego, CA, 385–387.

SEMALTIANOS, N.G., PERRIE, W., CHENG, J., FRENCH, P., SHARP, M., DEARDEN, G. & WATKINS, K.G. (2010). Picosecond laser ablation of nickel-based superalloy C263. *Appl. Phys. A* **98**, 345–355.

SEMALTIANOS, N.G., PERRIE, W., FRENCH, P., SHARP, M., DEARDEN, G., LOGOTHETIDIS, S. & WATKINS, K.G. (2009). Femtosecond laser ablation characteristics of nickel-based superalloy C263. *Appl. Phys. A* **94**, 999–1009.

TAN, B. & VENKATAKRISHNAN, K. (2006). A femtosecond laser-induced periodical surface structure on crystalline silicon. *J. Micromech. Microeng.* **16**, 1080–1085.

TRTICA, M.S., RADAK, B.B., GAKOVIC, B.M., MILOVANOVIC, D.S., BATANI, D. & DESAI, T. (2009). Surface modifications of Ti6Al4V by a picosecond ND:YAG laser. *Laser Part. Beams* **27**, 85–90.

ZYSK, K.T. (1990). Pulsed CO_2 laser welding of Inconel 718. *Proc. AIAA, SAE, ASME, ASEE 26th Joint Propulsion Conference*, **10**.